

**To study the effect of different drying techniques on functional properties and physicochemical properties of developed aerogel**

---

**4.1 Introduction**

In the recent times, corn starch has grabbed the attention of researchers as it is having broader range of application potential in the field of aerogel. However, structural collapse, poor mechanical strength, high stiffness etc. restricts the use of biopolymer-based aerogel in the food systems (Abdullah et al., 2022). Glycerol, which is having similar glucose unit to starch is very often used as plasticizer in starch. Starch molecule's intermolecular interaction is reduced due to addition of glycerol thereby results in increased intermolecular spacing which promotes flexibility and reduces fragility to the entire structure (Aghazadeh et al., 2018). Presence of glycerol also increases starch molecules affinity towards water due to increase in number of hydroxyl groups and it also helps in developing strong hydrogen bonds with water because of reduction in O-H band stretching (Aghazadeh et al., 2018; Nordin et al., 2020).

Generally, preparation of hydrogel and drying of the prepared hydrogel is the two main steps of aerogel development. However, sometime one additional step of alcogel preparation through sequential solvent (alcohols: ethanol, methanol, etc.) transfer into hydrogel is also required prior to drying of hydrogel. The drying process act as deciding factor whether the additional alcogel preparation is required or not. Moreover, the drying process of aerogel is very crucial as it regulates physicochemical properties (porosity, morphology, structural integrity, etc.) of aerogel which makes aerogel's definition ambiguous (Nita et al., 2020; Zheng et al., 2020). Generally, ambient pressure drying, vacuum drying, supercritical CO<sub>2</sub> drying, freeze drying, etc. are used in aerogel preparation. Among the aforesaid drying methods, freeze drying does not need any additional step of alcogel preparation. To the best of our knowledge, aerogel is a three-dimensional network of gels prepared by substitution of liquid with gas. Among the drying methods, freeze drying and supercritical CO<sub>2</sub> drying is widely used since last few years. Supercritical CO<sub>2</sub> drying is preferred due to its capability of maintaining gel structure and pores, producing smaller pores, lowering shrinkage rate, etc. However, supercritical CO<sub>2</sub> drying possesses some disadvantages like, time consuming, expensive, complex in operation, etc. Whereas freeze drying is recognized due to its unique characteristics like, simple in operation, economical, environment friendliness, etc. Moreover, freeze drying shows lowest shrinkage in aerogel in contrast with other techniques. However, freeze drying shows

disadvantages like, high energy consumption, long time-consuming process, chances of structural collapse of aerogel (Nita et al., 2020). To overcome those constraints of drying, microwave can be a good alternative as it is a rapid, simple, and environment friendly technique. Microwave imparts alternating electromagnetic field which causes rotation of liquid molecules and align their electric dipoles which promotes overall molecular vibration and thereby promotes their own heating. Therefore, high temperature heating cycle is also avoided (Durães et al., 2013). Microwave drying possesses some advantages like, smaller thermal gradients as it generates heat internally, fast and uniform heating, reduced drying time and energy consumption etc. (Durães et al., 2013).

A research gap on the development of corn starch-based aerogel using microwave and its characterization was observed after a brief literature review. Therefore, in this study we hypothesized to develop aerogel using microwave drying and comparing the quality parameters (physico-mechanical, morphological, functional, etc.) of aerogel with the aerogel developed by using freeze drying. Impact of glycerol on physico- functional, mechanical, morphological, and thermal characteristics of corn starch aerogel developed using both drying techniques has also been studied.

## **4.2 Materials and methods**

### **4.2.1 Materials**

Corn starch (amylose content: 13.32 %) was procured from LOBA CHEMIE PVT. LTD. Potassium chloride (KCl), calcium chloride ( $\text{CaCl}_2$ ), glycerol, and silica gel were purchased from Merck Life Science Private Limited (Mumbai, India). Ethyl alcohol ( $\text{C}_2\text{H}_5\text{OH}$ ) having more than 99.5 % purity was procured from Changshu Hongsheng Fine Chemical Co. Ltd (Changshu, Jiangshu, China).

### **4.2.2 Development of cylindrical aerogel**

The overall process of aerogel development consists of three steps which includes: (i) formation of hydrogel, (ii) formation of alcogel, and (iii) formation of aerogel. It is noteworthy mentioning that the development of freeze-dried aerogel does not require an additional step of alcogel preparation.

Hydrogel and alcogel was made by following the method described in section 3.2.2.1 and 3.2.2.2 respectively. Freeze drying and microwave drying were used to form aerogel from hydrogel and alcogel respectively. The pieces of hydrogel were freeze dried (LYOLAB, LYOPHILLIZATION SYSTEMS INC., USA) using a condenser temperature of  $-80\text{ }^{\circ}\text{C}$  and

pressure less than 100  $\mu\text{Hg}$  for 18 h (Fonseca et al., 2021). Whereas pieces of alcogel were dried using a commercial microwave oven operated at 240 W (surface temperature:  $73.85 \pm 1.10$   $^{\circ}\text{C}$ ) for 28 min. The conditions for microwave drying were selected on the basis of the results (**Fig. 4.1**) in terms of structure maintaining capability (no shape deformation, surface peel off and break in the structure) of the aerogel after preliminary experimental trials at different combination of power and time. To make sure about negligible traces of ethyl alcohol present in the dried samples, the samples were oven dried at 105  $^{\circ}\text{C}$  for 2 h and the amount of ethanol evaporated was measured at different time intervals (Ubeyitogullari & Ciftci, 2016; Zamora-Sequeira et al., 2018). The dried samples (FD0, FD5, FD7.5, FD10, MD0, MD5, MD7.5, and MD10; where, FD: freeze dried, MD: microwave dried, 0, 5, 7.5, and 10 represents 0 %, 5 %, 7.5 % and 10 % glycerol respectively) were stored properly in a desiccator (desiccant: silica gel) for further experiments.



**Fig. 4.1** Developed aerogel through microwave drying at different power level

### 4.2.3 Characterization

#### 4.2.3.1 Total percentage shrinkage, density, and porosity

##### 4.2.3.1.1 Total percentage shrinkage

Total percentage shrinkage ( $S_T$ ) was calculated on the basis of the difference in volume between hydrogel ( $V_{\text{hyd}}$ ) and aerogel ( $V_{\text{aer}}$ ). The volume of hydrogel ( $V_{\text{hyd}}$ ) and aerogel ( $V_{\text{aer}}$ ) was calculated by measuring the diameter and height of hydrogel and aerogel respectively. Total percentage shrinkage was calculated using **Eq. 4.1** (Q. Luo et al., 2019).

$$S_T(\%) = \frac{V_{\text{hyd}} - V_{\text{aer}}}{V_{\text{hyd}}} \times 100 \quad (4.1)$$

Where,  $S_T$ = total shrinkage percentage,  $V_{\text{hyd}}$ = volume of hydrogel,  $V_{\text{aer}}$ = volume of aerogel

##### 4.2.3.1.2 Density and porosity

To calculate the density ( $\rho$ ), mass of aerogel was divided by the volume of aerogel. Whereas the porosity ( $\epsilon$ ) of aerogel was determined by using the following equation (**Eq. 4.2**) (Ubeyitogullari et al., 2018).

$$\text{Porosity}(\%) = \left(1 - \frac{\rho}{\rho_{sk}}\right) \times 100 \quad (4.2)$$

Where,  $\rho$  = density of aerogel,  $\rho_{sk}$  = skeletal density of corn starch = 1.5 g/cm<sup>3</sup>.

#### 4.2.3.2 Morphology

To study the morphology, aerogel was cut into pieces of 10 mm diameter and 1 mm thickness. Then the pieces of aerogel were kept under vacuum and a thin layer of gold was spread on the top surface of the sample (J. P. de Oliveira et al., 2019). A scanning electron microscope (JEOL JSM-6390LV, Japan) was used to observe morphology of the sample under an accelerating voltage of 15 kV. The magnification set for the observation of sample's surface were 5,500 $\times$  and 10,000 $\times$ . A field emission scanning electron microscope (JEOL JSM-7200F, Japan) was also used to characterize morphology of the microwave dried control aerogel. The magnification was set to 40,000  $\times$  and 100,000  $\times$  to observe the sample surface.

#### 4.2.3.3 Mechanical performance and recompressibility

Mechanical performance and recompressibility test of aerogel was performed in Texture analyzer (TA-XD PLUS, Stable Micro System, UK) with a load cell of 30 kg. The test parameter was set to a pre-test and test speed of 1 mm/s and 0.1 mm/s respectively. Mechanical performance was measured in terms of compressive strength. To check the compressive strength, aerogel was subjected to 10, 20, 30, and 50 % strain at room temperature.

Recompressibility of aerogel was measured by subjecting the samples under repetitive compression test (loading-unloading compression) at a particular strain (50 %) for 10 times.

#### 4.2.3.4 Crystallinity

The aerogel samples were irradiated with an X-ray beam (30 kV voltage and 15 mA current) in an X-ray diffractometer (Miniflex, Rigaku Corporation, Japan). Diffraction angle ( $2\theta$ ) ranging from 5° to 80° with a step angle 0.05° were set. The degree of crystallinity was obtained after analysing the diffraction pattern. A smooth line connecting the lower points of XRD peaks was used to separate amorphous region from the crystalline region. Then, the area of crystalline region ( $A_C$ ) was calculated by integrating the area under the peaks. The total area ( $A_T$ ) under curve was calculated by integrating the curve over  $2\theta$  between 5° and 80° (Fonseca et al., 2021; Kumar et al., 2020). Degree of crystallinity was calculated by the following equation (Eq. 4.3):

$$\text{Degree of crystallinity}(\%) = \frac{A_C}{A_T} \times 100 \quad (4.3)$$

$A_C$  = area of crystalline region,  $A_T$  = total area under the curve

#### 4.2.3.5 Thermal behavior

Differential scanning calorimetry (DSC) was performed to characterize the thermal behavior. Approximately 5 mg sample was loaded and sealed in an aluminium pan and placed inside a differential scanning calorimeter (DSC 214, NETZSCH, Germany) for thermal scanning. Thermal scanning of aerogel samples was performed in the temperature range from 25 to 400 °C, at a heating rate of 10 °C/min, under a nitrogen purge (20 ml/min) (Franco et al., 2018).

#### 4.2.3.6 Hygroscopicity

For hygroscopicity, approximately 1 g of aerogel sample was taken in a PP (polypropylene) culture dish and placed inside a desiccator (relative humidity 85 %) at room temperature. Then, the weight of the sample was taken at an interval of 24 h till constant weight is achieved (Chen & Zhang, 2019). Hygroscopicity of the aerogel samples were measured by using the following equation (Eq. 4.4):

$$\text{Hygroscopicity} \left( \frac{\text{g}}{100\text{g}} \right) = \frac{M_g - M_0}{M_0} \times 100 \quad (4.4)$$

Where,  $M_0$ = initial weight of the sample and  $M_g$ = gained weight of the sample after every 24 h.

#### 4.2.3.7 Water absorption capacity

To study water absorption capacity at 30 min ( $\text{WAC}_{30 \text{ min}}$ ) and water absorption capacity (WAC), known weight ( $M_0$ ) of samples were kept inside a beaker having 20 ml of distilled water for 30 min and 24 h respectively. Then the samples were taken out from the beaker with the help of a forceps. Immediately after wiping off the surface water, the weight of the samples was taken. Then WAR and WAC was calculated by the following equations (J. P. de Oliveira et al., 2019; Lin et al., 2012) respectively (Eq. 4.5 and Eq. 4.6):

$$\text{WAC}_{30 \text{ min}}(\%) = \frac{M_w - M_0}{M_0} \times 100 \quad (4.5)$$

$$\text{WAC}(\%) = \frac{M_f - M_0}{M_0} \times 100 \quad (4.6)$$

Where,  $\text{WAC}_{30 \text{ min}}$ = water absorption capacity at 30 min,  $M_w$ = weight of wet sample after 30 min WAC= water absorption capacity,  $M_f$ = final weight of the sample,  $M_0$ = initial weight of the sample

#### **4.2.3.8 Reusability**

For repetitive water absorption ability of aerogel samples, the initial weight ( $M_0$ ) of the samples was taken and then, the samples were soaked in water for 30 min. The weight ( $M_w$ ) of the soaked samples was taken immediately after wiping off the surface water by a filter paper. Then the samples were placed inside a hot air oven at 45 °C for overnight drying till constant weight is achieved. The same process was repeated for eight times. The  $WAC_{30 \text{ min}}$  value was calculated by following **Eq. 4.5** during overall water absorbing and discharging process (Lin et al., 2012).

#### **4.2.4 Statistical analysis**

IBM SPSS (SPSS 17.0, SPSS Inc., Chicago, IL) software was used to perform statistical analysis. One-way ANOVA (analysis of variance) was performed to analyse the data. The one-way ANOVA was used to compare the means between the samples and determine whether the means of sample is significantly different from each other. It serve the purpose of identification whether the addition of glycerol has significant impact or not in the final properties (physico-functional, thermal, mechanical properties etc.) of the samples. Moreover, to know the variation among the samples for a particular quality characteristics of aerogel one way ANOVA was performed. To determine the statistical significance, the level of significance was set to  $p < 0.05$ . DMRT (DUNCAN'S multiple range test;  $p < 0.05$ ) test was performed to determine the significant difference among individual results. In addition to this Duncan Multiple Range Test (DMRT) was performed to know about the nature of variation whether it exhibits significant or non-significant difference between the mean values of samples with respect to all properties. Origin Pro 2018 (OriginLab, USA) software was used for graphing and principal component analysis (PCA). All the experiments were performed in triplicates and the results were represented as mean  $\pm$  standard deviation.

### **4.3 Results and discussion**

#### **4.3.1 Shrinkage and physical properties**

Total shrinkage percentage ( $S_T$ ) of aerogel are presented in **Fig. 4.2**. All hydrogel samples got after 48 h of aging showed no detectable shrinkage. However, noticable volume shrinkage was observed after conversion of hydrogel into aerogel. Significant difference ( $p < 0.05$ ) was observed between  $S_T$  values of Freeze and microwave dried aerogel. Moreover, significant difference ( $p < 0.05$ ) was also noticed between  $S_T$  values of glycerol added and control aerogel samples. The higher volume shrinkage was exhibited by the microwave dried samples in

comparison to the freeze-dried samples and it may be due to reduction in surface tension with the increase in ethanol concentration during solvent transfer process. Because of reduced surface tension capillary forces decreases which results in reversing direction of flow towards bulk solution from gel matrix that leads to decrease in gel volume (Mehling et al., 2009). The lesser  $S_T$  value was observed in case of control sample dried through freeze drying and microwave drying as compared to glycerol added samples. It is noteworthy mentioning that drying process leads to comparably lesser shrinkage than the solvent transfer process. The glycerol added sample exhibited significantly higher  $S_T$  values as compared to control samples of freeze and microwave dried aerogel (**Fig. 4.2**). The  $S_T$  values are progressively raised with the rise in glycerol concentration from 5 % to 10 %. In glycerol added samples changes in  $S_T$  values were observed due to shrinkage during freeze and microwave drying operation. A similar finding was also observed during supercritical drying of glycerol added aerogel which is reported in **section 3.3.2 of Chapter 3**. As the concentration of glycerol increases, the shrinkage values observed to be enhanced in the aerogel containing glycerol which may be due to reduction in surface tension within the aerogel matrix (García-González et al., 2012). Moreover, the affinity of glycerol toward O-H group leads to develop interconnected network which may results in higher shrinkage in glycerol added samples.

Density and porosity values (**Fig. 4.3**) of aerogel developed through freeze drying and microwave drying showed significant difference. Moreover, significant difference in density and porosity value was also observed between control and glycerol added samples. The density of freeze-dried aerogel raised with the rise in glycerol concentration from 5 % to 10 %. Significant difference was also observed between control and glycerol added samples dried through microwave drying. However, the density of microwave dried aerogel effected insignificantly by the glycerol level except for 5 % glycerol contained aerogel. Freeze dried samples showed higher porosity values as compared to the microwave dried samples. This may be due to development of tiny ice crystals within the hydrogel matrix which replace the water along with an increase in volume which contributes to the increased porosity of freeze-dried aerogel. Microwave irradiation causes volumetric heating through dipolar rotation of polar solvent. The generation of heat inside the structure may leads to shrink it more which results in developing compact structure of having high density. Moreover, shrinkage percentage plays an important role in regulating the density and porosity of aerogel, as higher shrinkage leads to form more compact structure with higher density and lesser porosity (Druel et al., 2017). The difference in density and porosity was significant between control and glycerol containing samples in case of both aerogel developed through different drying methods. However, the

change in porosity of freeze-dried aerogel was significant with the rise in glycerol concentration (5-10 %) whereas microwave dried samples showed insignificant changes. The density increment is closely amalgamated to porosity decrement. The addition of glycerol helps in the formation of thick and more connected network (efficient action of glycerol leads to hydrogen bond formation between polymer chains) within the aerogel matrix, may be attributed as the reason of increased density and reduced porosity of the aerogel (A. C. S. de Oliveira et al., 2021; Fontes-Candia et al., 2019; Ubeyitogullari et al., 2018). As shown in **Table 2.2** of **Chapter 2**, comparable physical properties of the developed corn starch-based aerogel are observed.

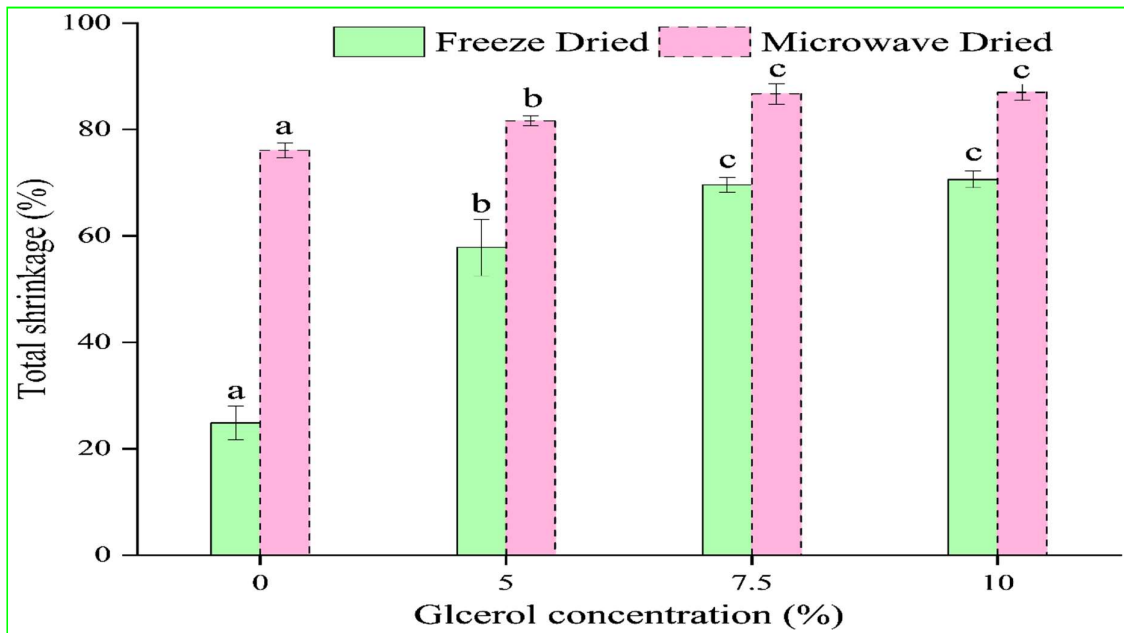


**Fig. 4.2** Total shrinkage of the freeze and microwave dried aerogel

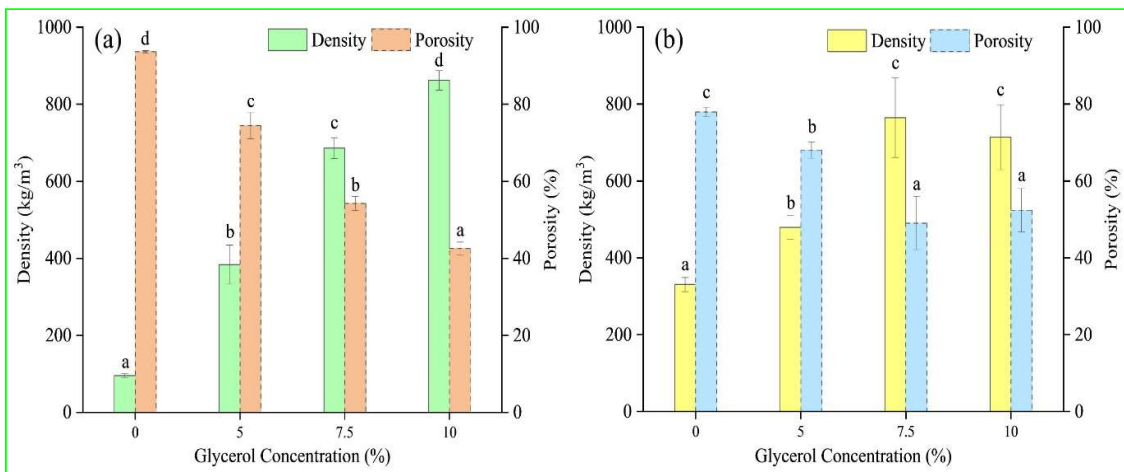


**Fig. 4.3** Density and porosity of freeze dried (a) and microwave dried (b) aerogel



### 4.3.2 Morphology

Aerogel developed through different drying methods showed different morphological properties (**Fig. 4.4** and **Fig. 4.5**). Specifically, the pores developed in freeze dried aerogel is comparatively bigger in size than the pores developed in microwave dried aerogel (**Fig. 4.4** and **Fig. 4.5**). The diameter of pores in microwave dried aerogel was found up to be approximately of 268 nm. Whereas, in case of freeze-dried aerogel the diameter of pores was up to 30  $\mu\text{m}$ . Control samples exhibited low density, high porosity, and thinner fibrils constituted network. The control aerogel developed through microwave drying showed more interconnected porous network with very small size pores (**Fig. 4.4a** and **Fig. 4.5b**) than the freeze dried control aerogel. However, addition of glycerol produced interconnected structure with thick fibrils connections (Ubeyitogullari et al., 2018). Freeze dried sample having 10 % glycerol (**Fig. 4.4**) showed thick interconnections with connected channel like pores. Moreover, number of small individual pores was found to be very less within the matrix of this aerogel. However, microwave dried aerogel having 10 % glycerol (**Fig. 4.5**) showed dense network with small size pores which is supported by physical properties (density and porosity; **Fig. 4.3**) of the aerogel. Moreover, the pore size distribution obtained from the FESEM images (**Fig. 4.6**) suggests that 5 % glycerol added aerogel exhibited more uniform and smaller pores than the control aerogel. This may be due to development of more organized structure as a consequence of glycerol addition.

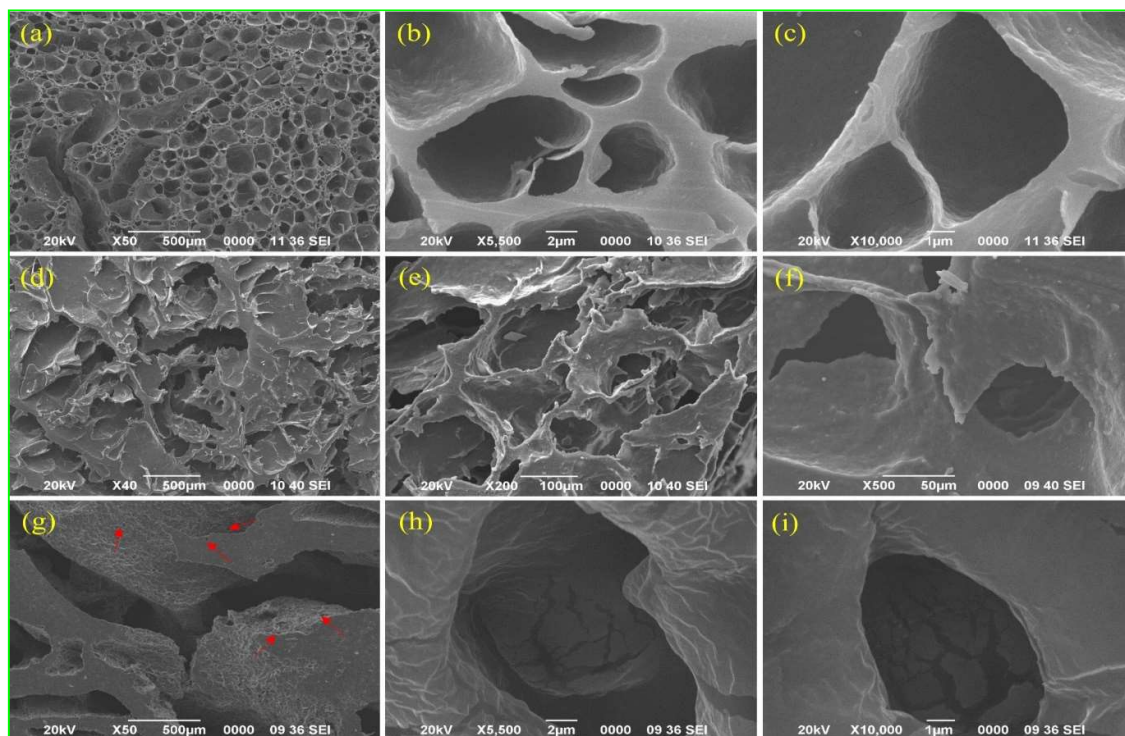


**Fig. 4.4** SEM images of control (a, b, & c), 5 % glycerol added (d, e, & f) and 10 % glycerol added (g, h, & i) freeze dried aerogel

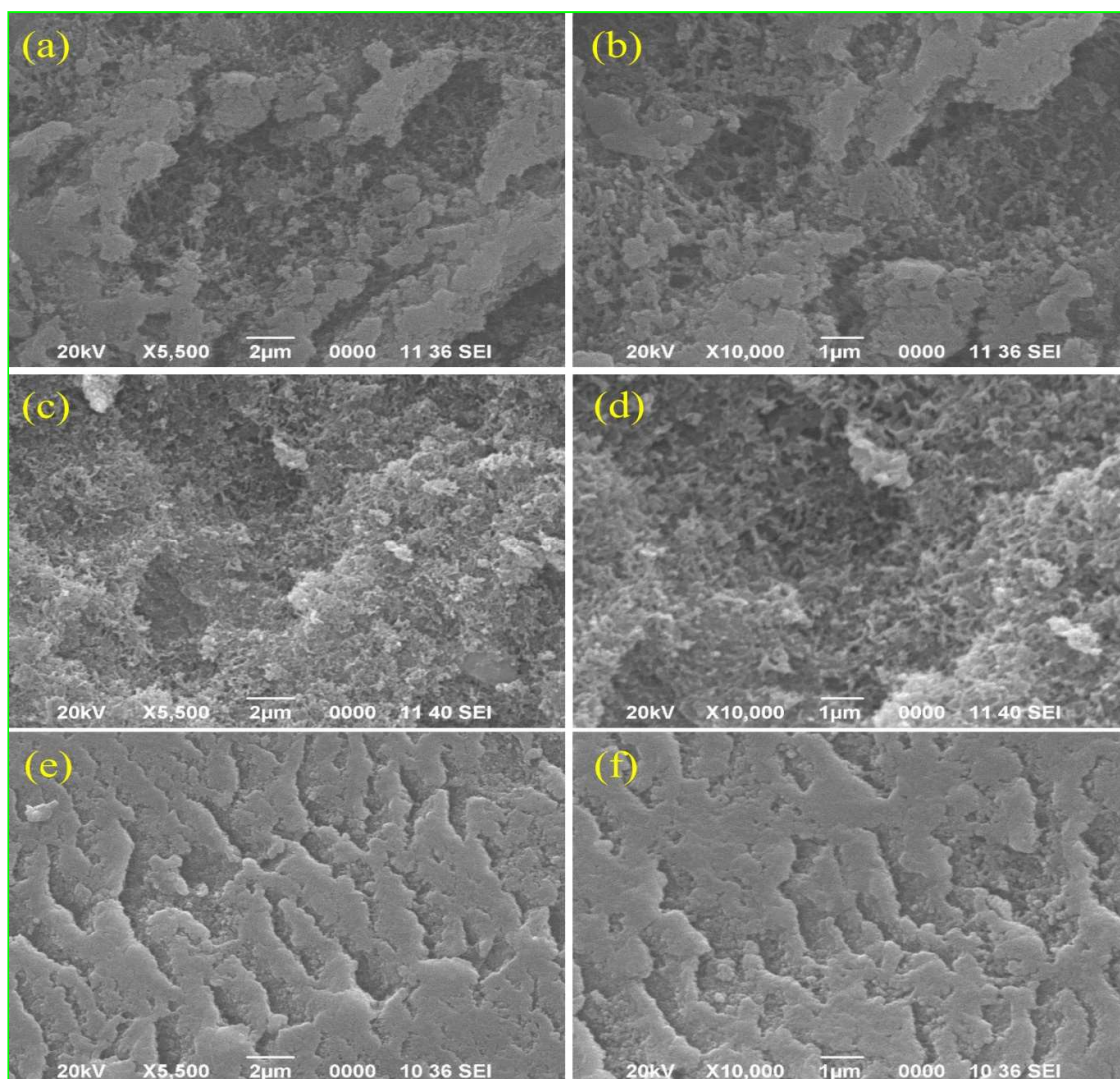


**Fig. 4.5** SEM images of control (a, & b), 5 % glycerol added (c & d) and 10 % glycerol added (e, & f) microwave dried aerogel

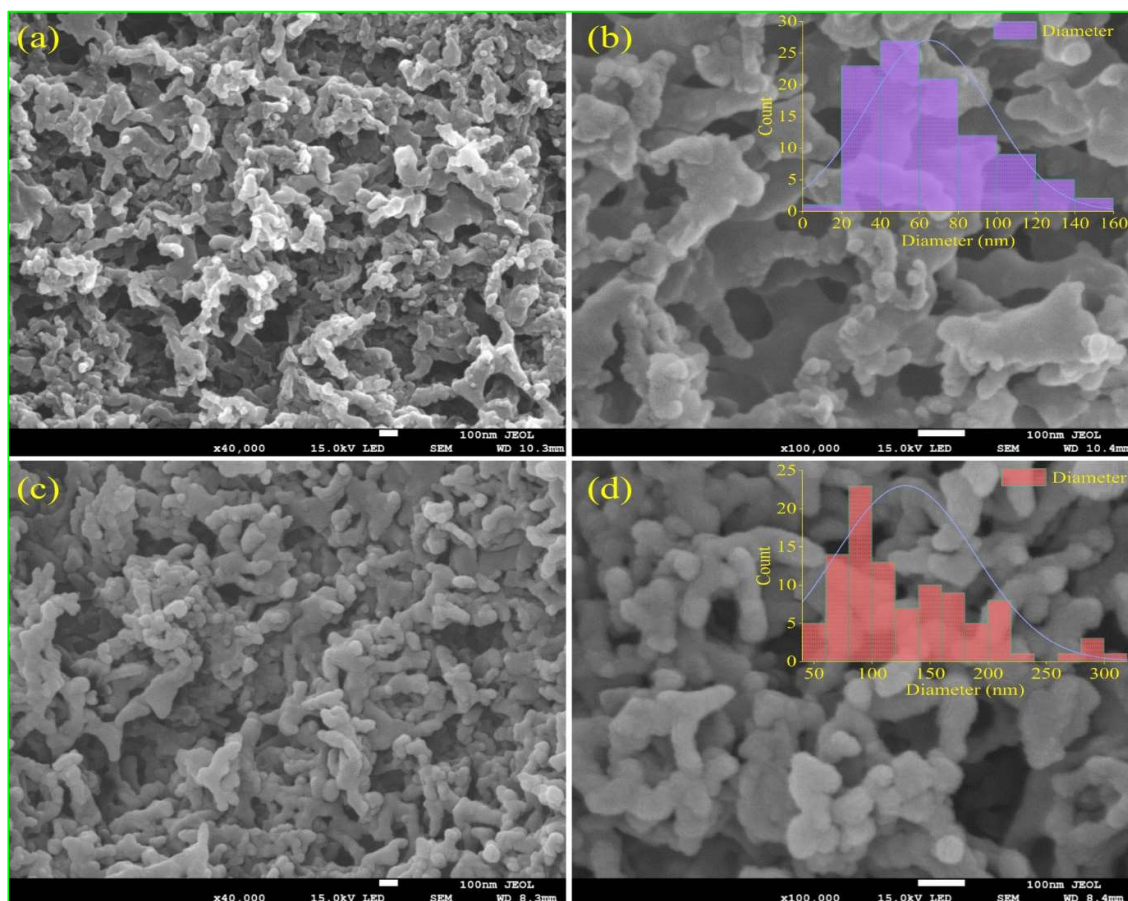


**Fig. 4.6** FESEM images of 5 % glycerol added (a, & b) and control (c & d) microwave dried aerogel

### 4.3.3 Mechanical properties

Compressive strength at different strain values and recompressibility study were performed to know the mechanical behaviour of the aerogel. Freeze dried and microwave dried aerogel showed different mechanical characteristics. The freeze-dried aerogel samples exhibited lesser compressive strength values at different strain as compare to the microwave dried aerogel samples. The control sample showed significantly high compressive strength in all strains as compared to glycerol added samples (**Fig. 4.7**). With the increase in glycerol concentration the compressive strength is decreased, that may be attributed as the reduction in firmness between the interconnections inside the aerogel matrix after addition of glycerol (Takeshita & Yoda, 2017). However, no significant difference in compressive strength was observed among glycerol added samples at any strain value. Significant difference ( $p < 0.05$ ) was observed in compressive strength at different strain for all the type of samples with an exception to the samples having lower glycerol concentrations (5 to 7.5 %). The evolvement in compactness of

structure during compression may results gradual increase in compressive strength with the rise in strain values. On the other hand, microwave dried aerogel exhibited opposite trend with lesser compressive strength value for the control sample (**Fig. 4.8**). Insignificant difference was observed in control sample as well as in 5 % glycerol added sample, when they subjected to lower strain (10 and 20 %). Moreover, with the increase in glycerol concentration, rise in compressive strength was observed. Addition of glycerol gave compact, denser structure, and so increased the stiffness of the aerogel network (Xiao et al., 2018; J. Zhu et al., 2019). The compressive strength can be correlated with the density and porosity values of the microwave dried aerogel. Bulk density and pore size plays an important role in regulating the mechanical toughness of aerogel (Takeshita & Yoda, 2017). Development of thick interconnections inside the aerogel matrix increases the density of both the aerogel. The bigger size and channel like pores (**Fig. 4.4**) with less firm thick connected walls in glycerol added freeze dried aerogel reduced it mechanical toughness whereas, the small pores with thick, firm, compact network of microwave dried glycerol added aerogel (**Fig. 4.5** and **Fig. 4.6**) provides it mechanical toughness.

Recompressibility test of aerogel was performed to examine the competency of aerogel to keep up it's structural integrity and texture during periodic compression and release experiment. It is observed that even after 10 cycles of loading-unloading, all the aerogel samples have retained their structure (**Fig. 4.9** and **Fig. 4.10**). During the initial stages of periodic loading-unloading, the compressive force decreased and thereafter no further noticable decrease in compressive strength was observed in all the aerogel (**Fig. 4.9** and **Fig. 4.10**). Decrease in compressive force may be due to breakdown of interconnections as a result of compression. Moreover, after a maximum possible breakdown in the interconnections, the structure become compact which may be attributed to the constant value of compressive strength during last few cycles of loading-unloading. The decrease in compressive strength in both freeze dried and microwave dried was comparatively high in control and aerogel with 5 % glycerol than the aerogel with 7.5 and 10 % glycerol (**Fig. 4.9** and **Fig. 4.10**). Breakdown in porous and organized network during compression may results in higher changes in compressive strength. However, the minor changes may suggest the capability of the aerogel to maintain its structural integrity. Decrease in compressive strength was found to be less in microwave dried aerogel, compact and dense structure of aerogel may resist the structural breakdown during compression.



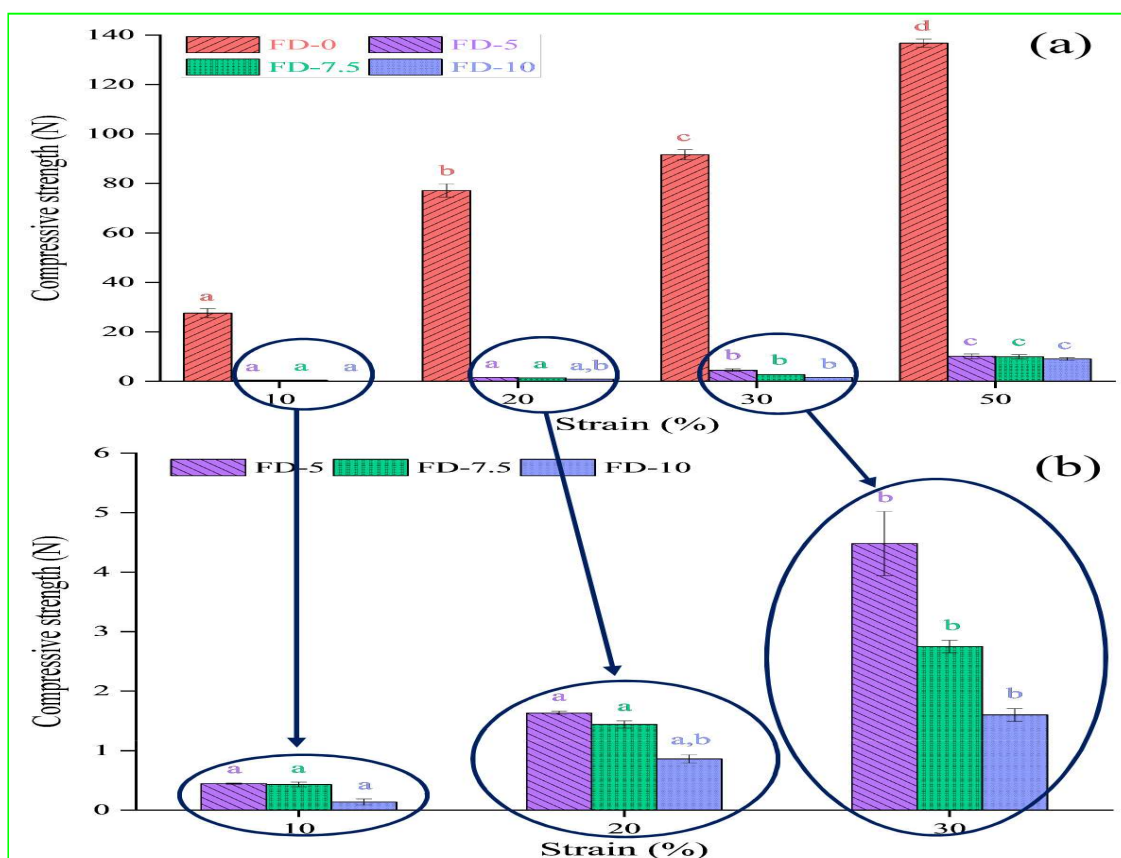


**Fig. 4.7** Compressive strength (a and b) of control (0) and glycerol added (5, 7.5, & 10 %) freeze dried (FD) aerogel

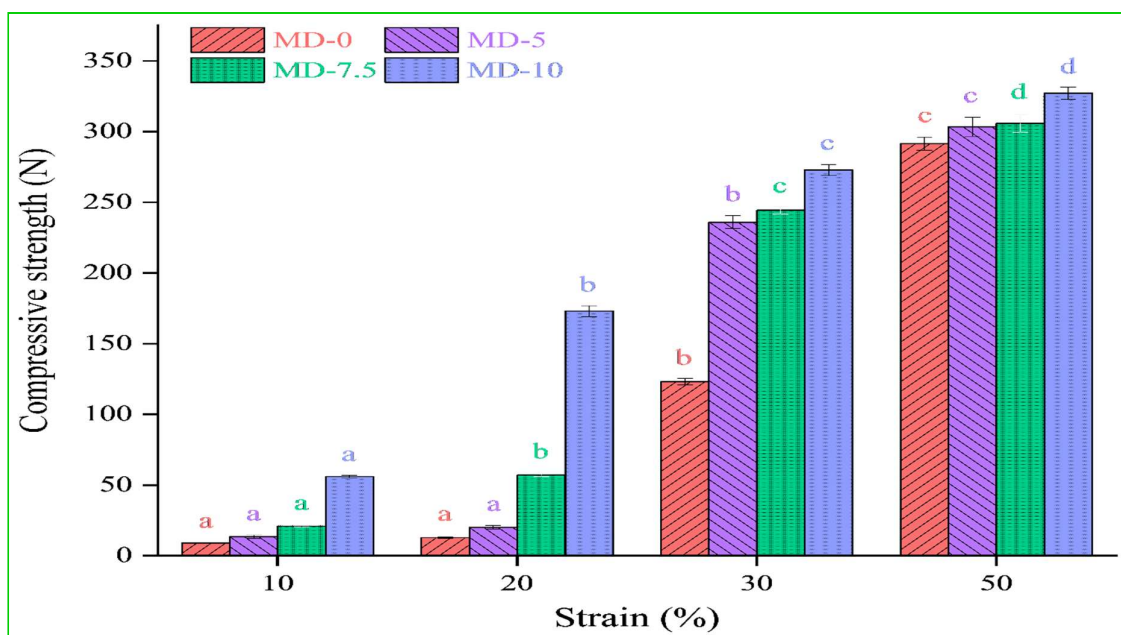


**Fig. 4.8** Compressive strength of control (0) and glycerol added (5, 7.5, & 10 %) microwave dried (MD) aerogel

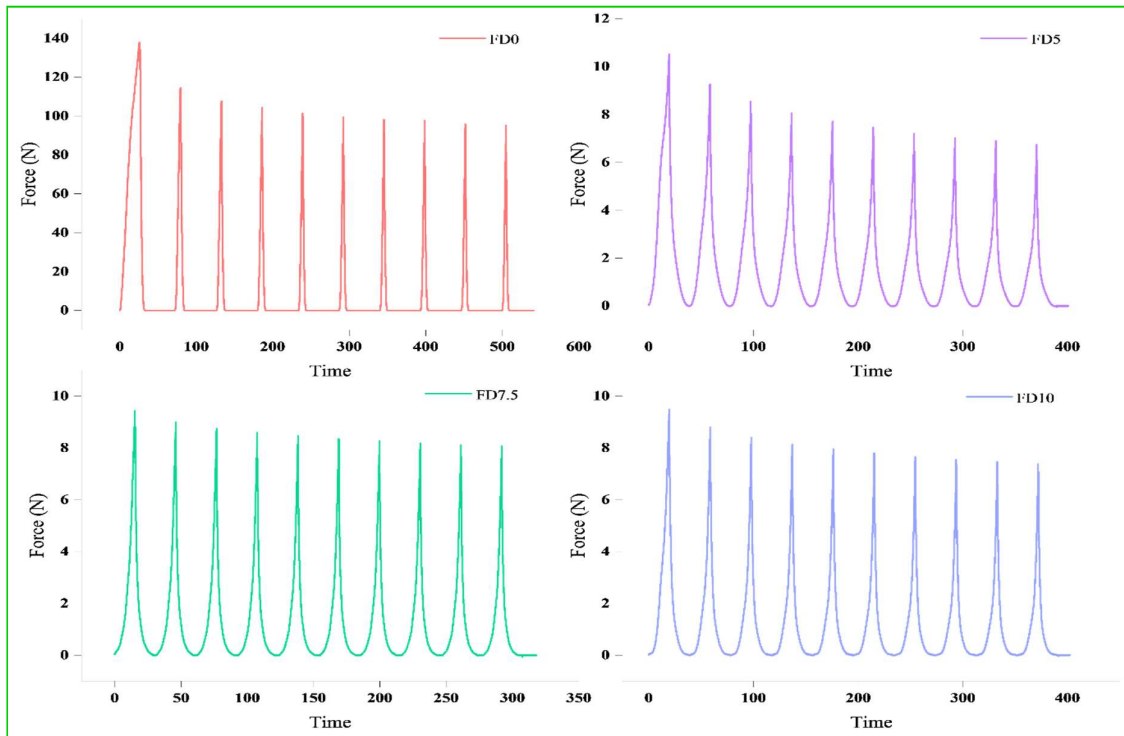


**Fig. 4.9** Recompressibility of control (0) and glycerol added (5, 7.5, & 10 %) freeze dried (FD) aerogel

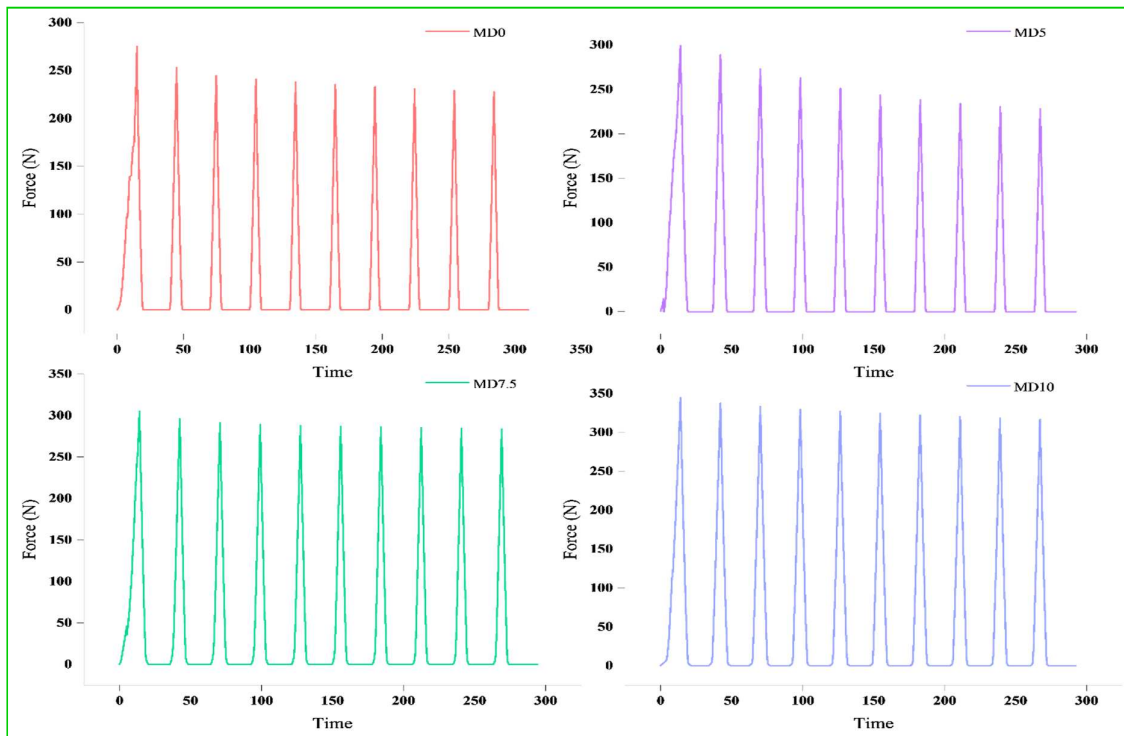


**Fig. 4.10** Recompressibility of control (0) and glycerol added (5, 7.5, & 10) microwave dried (MD) aerogel

#### 4.3.4 Crystallinity

Swelling of starch during gelatinization disrupts the crystallinity of starch, which further developed through reassociation of starch macromolecules during retrogradation (Aghazadeh et al., 2018). These two phases are exclusively related to production of aerogel. Therefore, the XRD diffractogram peaks are used to determine the value of starch crystallinity remained after aerogel formation (Fonseca et al., 2021; F. Zhu, 2019). The difference in hydrogen bond formation was also assessed through XRD technique. The figure indicates that it is a characteristic B-type XRD pattern (Kumar et al., 2020). Four major (approximately at  $2\theta = 17, 19, 21,$  and  $23^\circ$ ) and one minor ( $2\theta = 34^\circ$ ) diffraction peak was observed in all the aerogel (**Fig. 4.11** and **Fig. 4.12**) that indicates B-type polymorph and amylose-lipid complex formation which represents a crystalline structure (F. Zhu, 2019). Presence of an additional peak at about  $2\theta = 13^\circ$  in glycerol added microwave dried aerogel (**Fig. 4.12**), suggests formation of amylose-lipid complex (Ubeyitogullari et al., 2018). The crystallinity index (CI) of freeze dried and microwave dried aerogel ranges from 21.68 to 41.24 % and 20.02 to 43.05 % respectively (**Fig. 4.11** and **Fig. 4.12**). The control samples of freeze and microwave dried aerogel showed lowest CI value i.e. 21.68 and 20.02 % respectively. Microwave treatment for a longer duration resulted in slight diffraction or disappearance and reduced intensity of peaks. This may be due reorganization of double helices towards amorphous form. Another reason of decreased crystallinity in microwave dried control aerogel may be the active hydroxyls formed due to breakdown of water molecules because of microwave treatment for long duration (Kumar et al., 2020). It is observed that the glycerol added sample had higher value of CI than the control samples irrespective of the drying methods. Addition of glycerol leads to crystallite development due to increase in starch chain mobility because of increase in open volume inside the polymer assembly of corn starch (Aghazadeh et al., 2018). Polymer crystals alignment may be increased by addition of glycerol which leads to form more orderly and crystalline region with intense peaks. With the increase in glycerol concentration CI value is also increased. This may be attributed to build up of interconnected network as a result of polymer network reorganization as a consequence of strong interconnection between polymers and glycerol within the aerogel matrix (Abhari et al., 2017; Liu et al., 2013). A similar increase in CI value was reported by Abhari et al. (2017) for citric acid cross-linked gel samples.

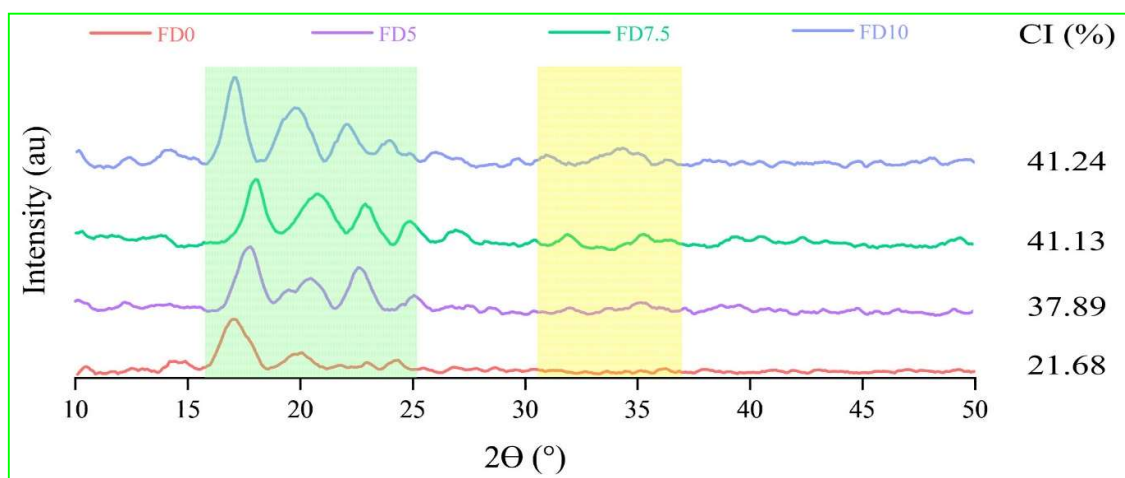


**Fig. 4.11** X-ray diffraction pattern and crystallinity index (CI) of control (0) and glycerol added (5, 7.5, & 10) freeze dried (FD) aerogel

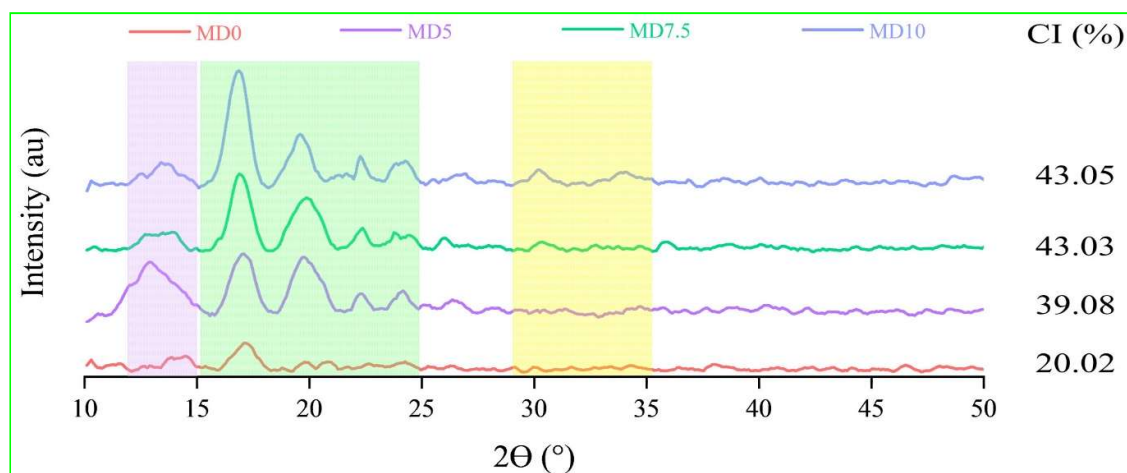


**Fig. 4.12** X-ray diffraction pattern and crystallinity index (CI) of control (0) and glycerol added (5, 7.5, & 10) microwave dried (MD) aerogel

#### 4.3.5 Thermal properties

The solid-state behaviour of the aerogel was studied by performing DSC analysis. The thermal behaviour was explained by representing the data (**Table 4.1**) of first endothermic peak obtained in DSC analysis. This characteristic endothermic peak (called as gelatinization temperature) may be attributed to the dehydration and gelatinization of aerogel (De Marco et al., 2015; Franco et al., 2018). The onset temperature ( $T_o$ ) and peak temperature ( $T_p$ ) was found higher in glycerol added freeze dried aerogel whereas, the end temperature ( $T_e$ ) was found to be lower than the control aerogel. The lowest concentration of glycerol (5 %) showed highest values of  $T_o$  (49.4 °C) and  $T_p$  (77.9 °C). In microwave dried aerogel, the  $T_o$  value exhibited by



lowest glycerol containing aerogel was higher and  $T_p$  value was found to be higher in 10 % glycerol containing aerogel.  $T_e$  value was found to be approximately same in 7.5 % and 10 % glycerol added aerogel. The increase in  $T_o$  may reflect the melting of weakest crystallites whereas the increase in  $T_e$  reflects the formation of crystallites having higher melting point (Z. Luo et al., 2006). The rise in  $T_p$  may be due to association of amorphous amylose in granular structure with enhanced stability (Stevenson et al., 2005). The increase in glycerol concentration leads to decrease in gelatinization enthalpy ( $\Delta H$ ) of both freeze ( $432.0 < 286.9 < 223.3$  J/g) and microwave dried ( $282.3 < 225.8 < 195.6$  J/g) aerogel. However, the freeze and microwave dried control aerogel exhibits  $\Delta H$  of 377.4 and 230.5 J/g respectively. The increase in  $\Delta H$  at low glycerol concentration (5 %) may be due to antiplasticization effect of glycerol. The possible reason behind this behaviour could be the development of strong network between starch and glycerol through hydrogen bonding which strengthened the polymeric network and develops aerogel with higher thermal stability (Chen & Zhang, 2019; Liu et al., 2013). The decrease in  $\Delta H$  with the increase in glycerol concentration could be due to plasticization effect of glycerol in the polymeric network of starch (Liu et al., 2013). It is also observed that  $\Delta H$  of microwave dried aerogel is significantly lesser than freeze dried aerogel. The decrease in  $\Delta H$  may be attributed to disruption of double helices present in crystalline and non-crystalline region due to microwave irradiation. In B-type starch packing of double helices is less compact hence, it is having high mobility and susceptibility towards disruption (Luo et al., 2006).

**Table 4.1** Thermal properties of freeze and microwave dried aerogel

Drying Method	Glycerol concentration (%)	Onset temperature (° C)	Peak temperature (° C)	End Temperature (° C)
Freeze	0	37.4	72.5	114.1
	5	49.4	77.9	105.2
	7.5	42.6	75.0	108.0
	10	43.2	77.5	111.9
Microwave	0	38.6	70.5	106.4
	5	45.0	79.7	140.3
	7.5	37.1	79.2	163.4
	10	38.7	83.0	163.3

#### 4.3.6 Hygroscopicity

Hygroscopicity of aerogel samples were studied for 10 consecutive days (Fig. 4.13) to know the moisture taking capability of aerogel from the surrounding environment. The composition and porosity of aerogel regulates the moisture gain from the humid environment (Arboleda et al., 2013). Aerogel samples dried through freeze drying and microwave drying showed

different behaviour during hygroscopicity study (**Fig. 4.13a** and **Fig. 4.13b**). The value of hygroscopicity of freeze-dried aerogel was higher than the microwave dried aerogel. Freeze drying leads to develop highly porous structure than the microwave dried aerogel samples which increases the chances of moisture migration through the pores. Addition of glycerol also plays an important role on regulating the hygroscopic behaviour of aerogel. The glycerol added sample showed higher hygroscopicity than the control sample in both freeze and microwave dried aerogel (**Fig. 4.13a** and **Fig. 4.13b**). This may be ascribed to congenital proclivity of glycerol and starch towards water. It may also be attributed to the increase in free volume as well as the increase in inter-chain spacing within the polymer matrix due to inclusion of glycerol which regulates the moisture diffusion inside aerogel matrix (Arboleda et al., 2013; Chen & Zhang, 2019; Ollé Resa et al., 2014). The hygroscopicity of freeze-dried aerogel increases with the increasing concentration of glycerol however in case of microwave dried aerogel, the sample containing 5 % glycerol showed highest hygroscopicity value which may be due to combined outcome of aerogel's porosity and glycerol. The accretive hygroscopic behaviour observed in freeze dried aerogel is supported by their porous structure and glycerol concentration.

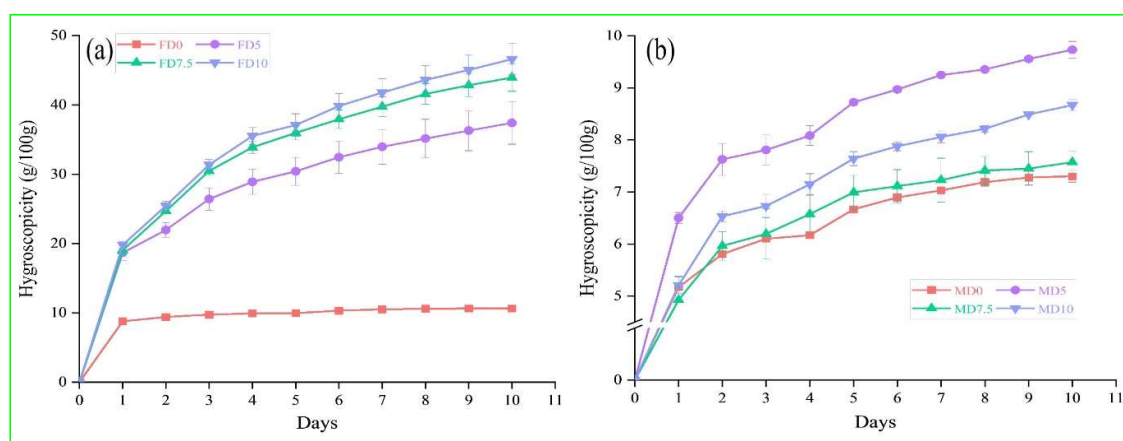


**Fig. 4.13** Hygroscopic behaviour of freeze dried (a) and microwave dried aerogel (b)

#### 4.3.7 Water absorption capacity (WAC)

Freeze and microwave dried aerogel showed different results in  $WAC_{30 \text{ min}}$  as well as in  $WAC_{24 \text{ h}}$  (**Fig. 4.14**). Significant difference in  $WAC_{30 \text{ min}}$  was observed between all the (control and glycerol added) samples of freeze-dried aerogel whereas microwave dried aerogel exhibited insignificant difference between all the glycerol added samples however, significant difference was observed between control and glycerol added aerogel (**Fig. 4.14**). Similar results as in case of microwave dried aerogel were observed in our previous study of super-critically

dried corn starch aerogel reported in **section 3.3.8 of Chapter 3**. Control samples of freeze dried and microwave dried aerogel showed highest  $WAC_{30 \text{ min}}$  in comparison to the glycerol added samples. The porous matrix of control samples allows quick water intake by the capillaceous structure due to less compactness whereas, the compact and dense structure of glycerol added aerogel restricts rapid water uptake through the capillary network. Porosity and density of the samples supports the same. Moreover, noticeable difference in  $WAC_{30 \text{ min}}$  value of freeze-dried samples (**Fig. 4.14a**) was observed as compared to respective microwave dried samples (**Fig. 4.14b**). This may be attributed to less compact and highly porous structure of freeze-dried aerogel.

Water absorption process in aerogel depends upon on the amount of vacant spaces present inside the internal matrix however, the capacity of water entrapment and absorption is also regulated by the density of the aerogel matrix (Fonseca et al., 2021). Freeze dried aerogel showed higher  $WAC_{24 \text{ h}}$  than the microwave dried aerogel and it may be due to the porous texture of the internal matrix. Significant difference in  $WAC_{24 \text{ h}}$  values were observed in all the samples of freeze and microwave dried aerogel (**Fig. 4.14a** and **Fig. 4.14b**). A decreasing trend in  $WAC_{24 \text{ h}}$  values was observed with the increase in glycerol concentration as it leads to develop more dense structure with lesser quantity of pores. This may be supported by the claim made by Fonseca et al. (2021). The density, porosity, and SEM images of the developed aerogel supports the same. Moreover, it was observed that the microwave dried aerogel containing 10 % glycerol showed higher  $WAC_{24 \text{ h}}$  (161.48 %) than the aerogel containing 7.5 % glycerol (144.03 %). This may be due to glycerol's affinity towards water and increased water holding ability due to presence of higher number of hydroxyl groups because of addition of glycerol in higher amount (Nordin et al., 2020). The  $WAC_{24 \text{ h}}$  values of the developed aerogel is also compared with some other studies (**Table 2.2 of Chapter 2**).

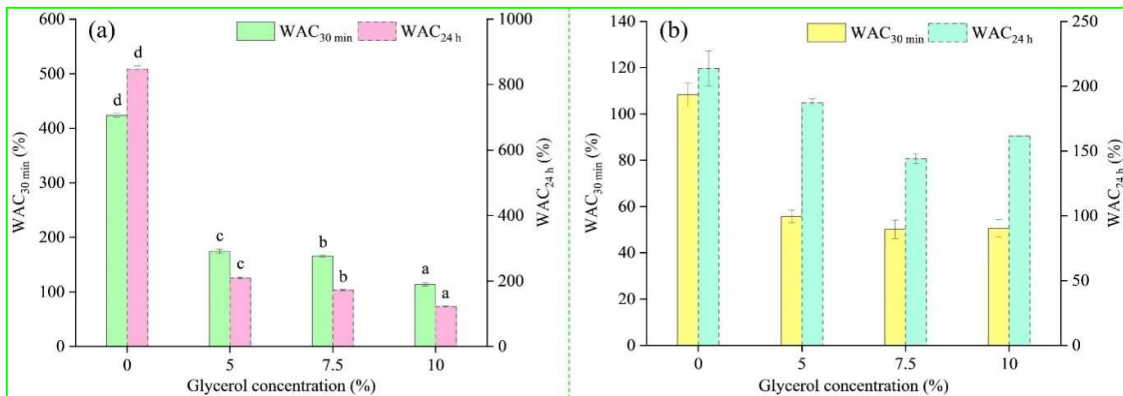


**Fig. 4.14** Water absorption capacity at 30 min ( $WAC_{30 \text{ min}}$ ) and 24 h ( $WAC_{24 \text{ h}}$ ) of freeze dried (a) and microwave dried aerogel (b)

### 4.3.8 Reusability

Reusability is a measure of structural stability of aerogel when it is subjected to periodic water absorption-desorption process. The 7.5 and 10 % glycerol added freeze dried aerogel resisted only 4 consecutive water absorption-desorption process (**Fig. 4.15**). The addition of glycerol at higher concentration leads to development of channel like porous structure (supported by the SEM images) within the aerogel matrix which may be attributed as the reason of structural collapse after four times of iterative water absorbing-discharging process. However, the other two (control and 5 % glycerol added) freeze dried aerogel resisted eight times of consecutive water absorption-desorption process. This may be due to presence of homogenous distribution of tiny pores which results in higher interconnections within the structural matrix. Moreover, all the microwave dried aerogel showed stability even after 8 times of repetitive water absorbing-discharging process (**Fig. 4.16**). This may be due to the compact and dense structure of the microwave dried aerogel. All the sample have showed decreased water absorption values after the first water absorbing-discharging process. However, all the freeze-dried samples showed slightly increased water absorption values after second water absorbing-discharging process, which may be attributed to the structural collapse of the internal matrix. The continuous decrease in water absorption values of all microwave dried aerogel may be due to shrinkage takes place after each discharging process.

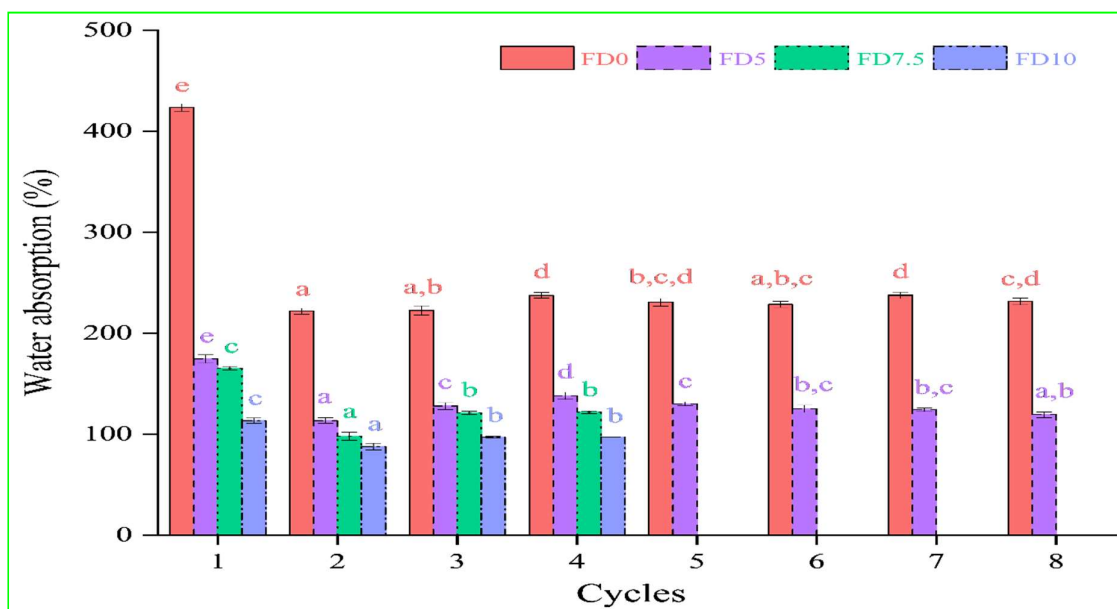


**Fig. 4.15** Reusability of control (0) and 5, 7.5, & 10 % glycerol added freeze dried (FD) aerogel

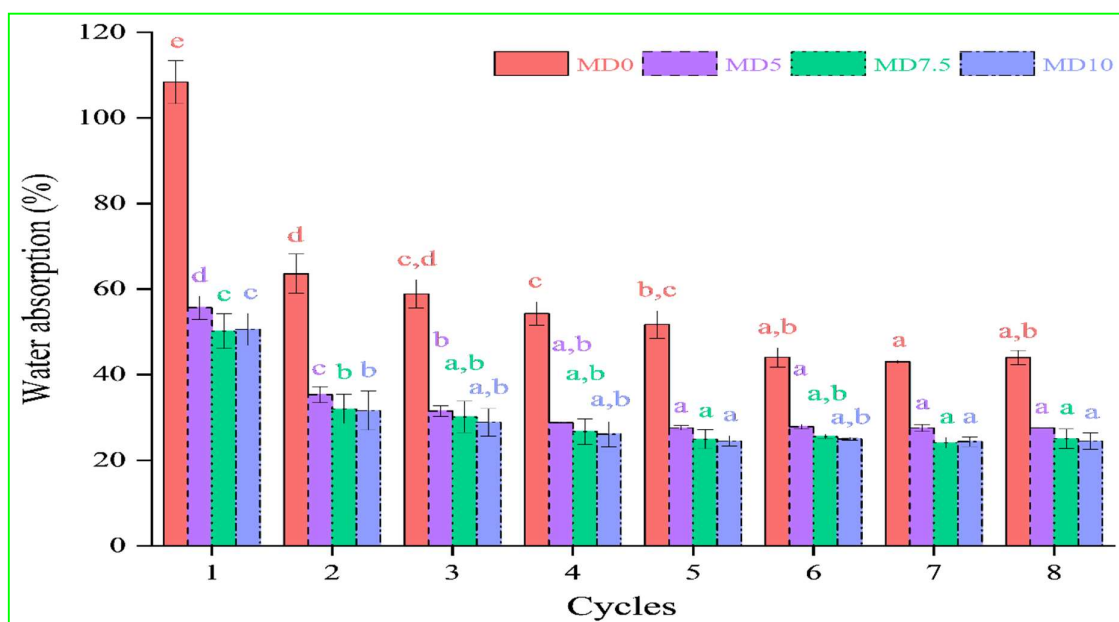


**Fig. 4.16** Reusability of control (0) and 5, 7.5, & 10 % glycerol added microwave dried (MD) aerogel

#### 4.3.9 Principal component analysis (PCA)

Principle component analysis (PCA) was performed to visualize the impact of drying method and glycerol concentration on quality attributes of different aerogel. More specifically, in present study PCA was used to show the correlation between the properties represented by the term loading plot whether they exhibited a positive correlation or a negative correlation with the other or with a cluster of properties existing near a score. The scores present on the figures depicted the samples having different concentration of glycerol. Moreover, this study present the properties (loading plot) nearly associated with a sample (score). How the effect of glycerol and drying method regulated the properties (physico-functional, thermal, and mechanical properties) of aerogel and the respective trends corresponds to the each sample was in line with the position of scores and loading plot in the PCA biplot. The PCA was performed without any pre-processing of data using 8 number of samples (FD: freeze dried, MD: microwave dried, control aerogel represented by '0', 5%, 7.5%, and 10% glycerol-based aerogel represented by '5', '7.5', and '10' respectively.) and 15 numbers of variables (ST- total % shrinkage,  $\rho$ - density,  $\epsilon$ - porosity, WAC- water absorption capacity, WAR- water absorption rate, CI- crystallinity index (%), CS10, CS20, CS30, and CS50 are compressive strength against 10, 20, 30, and 50% strain respectively,  $T_i$ ,  $T_f$ ,  $T_o$ ,  $T_p$ , and  $T_e$  are initial, final, onset, peak, and end temperature respectively) which is represented in the biplot as scores and loading plot respectively. The algorithm used in PCA of the present study was Eigen-decomposition of

the covariance/correlation matrix. The biplot (**Fig. 4.17**) obtained from PCA was used to represents the variations (81.59 %) to correlate scores (drying methods and glycerol concentration) with loadings (properties). The scores discriminate the samples treated differently by the position and distance from the centre based on the physico-functional, mechanical, and thermal properties given in the loading plot. All the properties distributed in the space of biplot is demonstrated by loading plot. Loading plots situated in inverse direction to each other corresponds positive and negative interrelation. However, orthogonal loading plots impart no correlation. Maximum number of characteristics are accompanied with glycerol containing microwave dried aerogel represented by two clusters (corresponds to MD5, MD7.5, and MD10). Moreover, cluster corresponds with control samples exhibited a negative interrelation on the characteristics like, porosity ( $\epsilon$ ), WAC<sub>24h</sub>, and WAC<sub>30 min</sub>. Microwave dried glycerol added samples located away from the freeze-dried samples due to their higher content of density, total shrinkage, thermal and mechanical properties as well as lower content of porosity and water absorption properties as compared to freeze dried samples.

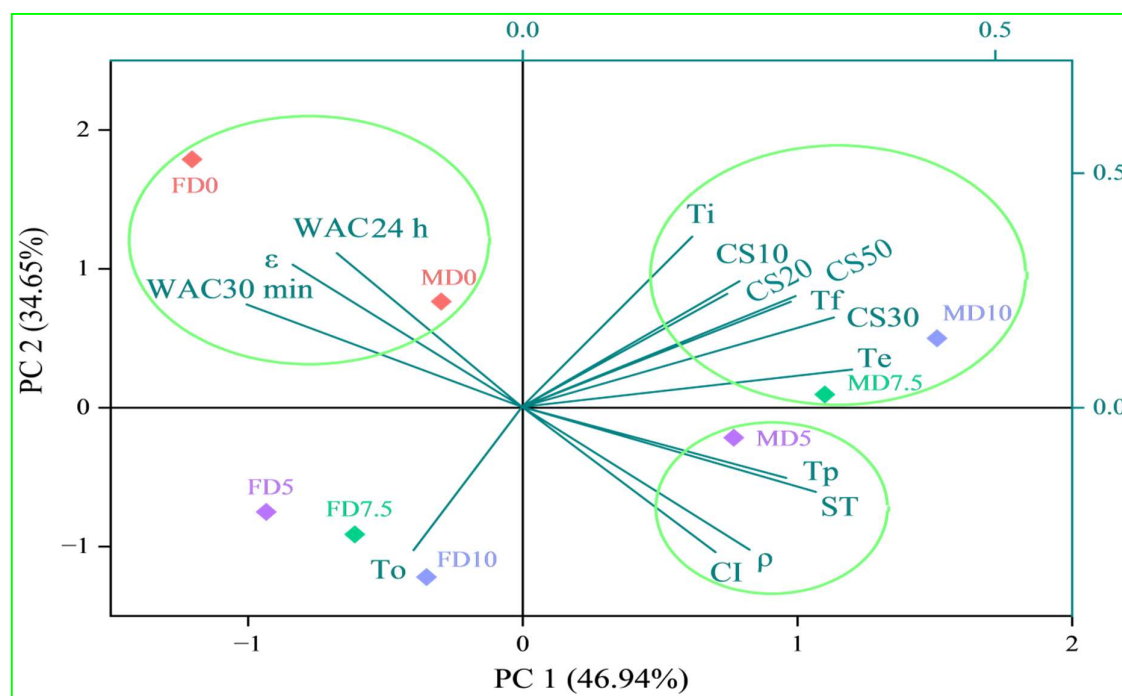


**Fig. 4.17** Principal component analysis (PCA) bi-plot of the characteristics of freeze dried (FD) and microwave dried (MD) aerogel

#### 4.3.10 Comparative study of standardized SCCO<sub>2</sub>, freeze, and microwave dried aerogel

Based on the physico-functional, morphological, and mechanical properties, 5 % glycerol based aerogel was standardized for SCCO<sub>2</sub> and microwave dried aerogel whereas, control

aerogel was selected as standard aerogel for freeze dried aerogel. Further, the aforesaid properties were compared for all the standardized aerogel and 5 % glycerol based microwave dried aerogel was selected as optimum aerogel for accomplishing the next objectives (**Table 4.2**). The selected aerogel exhibited comparable physico-functional and mechanical properties to SCCO<sub>2</sub> dried aerogel. Moreover, the microwave dried aerogel exhibited good morphology in terms of uniform nano range pores inside the aerogel matrix and it is suitable for CDs based nanomaterial applications. Nevertheless, the SCCO<sub>2</sub> dried aerogel exhibited porous fibril network of higher pore size as compare to microwave dried aerogel. Although the freeze dried control aerogel exhibited better physico-functional properties compare to other aerogel however, it lacked the mechanical strength and nano-porous structure (**Table 4.2**). Beside the aforementioned properties, microwave drying possesses other advantages like, operational simplicity, less time consuming, economic, sustainable, environment friendly, etc. which also supported the selection of microwave dried aerogel for further analysis.

**Table 4.2** Physico-functional and mechanical properties of standardized SCCO<sub>2</sub>, freeze and microwave dried aerogel

Sample	Density (kg/m <sup>3</sup> )	Porosity (%)	WAC <sub>24 h</sub> (%)	WAC <sub>30 min</sub> (%)	Compressive strength (N) at different strain (%)			
					10	20	30	50
SCD5	381.08	74.59	211.85	89.63	24.60	77.13	183.72	211.30
MD5	479.34	68.04	187.33	55.66	13.40	19.98	235.91	303.44
FD0	95.37	93.64	847.81	423.64	27.54	77.15	91.60	136.75

# SCD5: supercritical CO<sub>2</sub> dried 5 % glycerol based aerogel; MD5: microwave dried 5 % glycerol based aerogel; FD0: freeze dried aerogel without glycerol

#### 4.4 Conclusion

The result of our study suggests the successful development of thin aerogel monoliths through microwave drying and freeze-drying approach. This study also includes impact of glycerol addition on physical, functional, mechanical, morphological, and thermal characteristics of microwave and freeze-dried aerogel respectively. Microwave and freeze drying have influenced aerogel's final properties differently. Freeze dried aerogel showed higher porosity, WAC<sub>24 h</sub>, WAC<sub>30 min</sub>, and low density than microwave dried aerogel. Whereas, microwave dried aerogel exhibited better reusability, mechanical and thermal stability than

freeze dried aerogel. Microwave drying possesses several advantages over freeze drying in terms of economic feasibility, ease of operation, less power consumption and short treatment time.

Amalgamation of glycerol improves internal network, CI, hygroscopicity, mechanical and thermal stability of aerogel however, it reduces the porosity of aerogel by developing dense structure. These properties are very crucial for an aerogel which helps to decide the area of its potential application like moisture scavenging, sensing, smart packaging, etc. Microwave drying is having several advantages like lesser time of operation, easiness in operation, simple, affordable, sustainable, novel, environment friendly, etc. on instrumental point of view and from product (aerogel) point of view, microwave drying resulted a light aerogel having good porosity and morphology with high mechanical strength. The 5 % glycerol based microwave dried aerogel was selected for further experiments. Microwave drying is an important technology in aerogel development and due to the nano-range pores, microwave dried aerogel can be used in pharma, functional food, bioactive compound carrier and delivery systems. Further study in the development of functional microwave dried aerogel is required which can reveal more new insights on it.

#### 4.5 References

- Abdullah, Zou, Y. C., Farooq, S., Walayat, N., Zhang, H., Faieta, M., Pittia, P., & Huang, Q. (2022). Bio-aerogels: Fabrication, properties and food applications. *Critical Reviews in Food Science and Nutrition*, 63(24), 6687-6709.
- Abhari, N., Madadlou, A., & Dini, A. (2017). Structure of starch aerogel as affected by crosslinking and feasibility assessment of the aerogel for an anti-fungal volatile release. *Food Chemistry*, 221, 147–152.
- Aghazadeh, M., Karim, R., Rahman, R. A., Sultan, M. T., Johnson, S. K., & Paykary, M. (2018). Effect of glycerol on the physicochemical properties of cereal starch films. *Czech Journal of Food Sciences*, 36(5), 403–409.
- Arboleda, J. C., Hughes, M., Lucia, L. A., Laine, J., Ekman, K., & Rojas, O. J. (2013). Soy protein-nanocellulose composite aerogels. *Cellulose*, 20(5), 2417–2426.
- Chen, K., & Zhang, H. (2019). Alginate/pectin aerogel microspheres for controlled release of proanthocyanidins. *International Journal of Biological Macromolecules*, 136, 936–943.
- De Marco, I., Baldino, L., Cardea, S., & Reverchon, E. (2015). Supercritical gel drying for the



- production of starch aerogels for delivery systems. *Chemical Engineering Transactions*, *43*, 307–312.
- de Oliveira, A. C. S., Ugucioni, J. C., & Borges, S. V. (2021). Effect of glutaraldehyde/glycerol ratios on the properties of chitosan films. *Journal of Food Processing and Preservation*, *45*(1), 0–3. <https://doi.org/10.1111/jfpp.15060>
- de Oliveira, J. P., Bruni, G. P., el Halal, S. L. M., Bertoldi, F. C., Dias, A. R. G., & Zavareze, E. da R. (2019). Cellulose nanocrystals from rice and oat husks and their application in aerogels for food packaging. *International Journal of Biological Macromolecules*, *124*, 175–184.
- Druel, L., Bardl, R., Vorwerk, W., & Budtova, T. (2017). Starch Aerogels: A Member of the Family of Thermal Superinsulating Materials. *Biomacromolecules*, *18*(12), 4232–4239.
- Durães, L., Matias, T., Patrício, R., & Portugal, A. (2013). Silica based aerogel-like materials obtained by quick microwave drying. *Materialwissenschaft Und Werkstofftechnik*, *44*(5), 380–385.
- Fonseca, L. M., Silva, F. T. da, Bruni, G. P., Borges, C. D., Zavareze, E. da R., & Dias, A. R. G. (2021). Aerogels based on corn starch as carriers for pinhão coat extract (*Araucaria angustifolia*) rich in phenolic compounds for active packaging. *International Journal of Biological Macromolecules*, *169*, 362–370.
- Fontes-Candia, C., Erboz, E., Martínez-Abad, A., López-Rubio, A., & Martínez-Sanz, M. (2019). Superabsorbent food packaging bioactive cellulose-based aerogels from *Arundo donax* waste biomass. *Food Hydrocolloids*, *96*, 151–160.
- Franco, P., Aliakbarian, B., Perego, P., Reverchon, E., & De Marco, I. (2018). Supercritical Adsorption of Quercetin on Aerogels for Active Packaging Applications. *Industrial and Engineering Chemistry Research*, *57*(44), 15105–15113.
- García-González, C. A., Uy, J. J., Alnaief, M., & Smirnova, I. (2012). Preparation of tailor-made starch-based aerogel microspheres by the emulsion-gelation method. *Carbohydrate Polymers*, *88*(4), 1378–1386.
- Kumar, Y., Singh, L., Sharanagat, V. S., Patel, A., & Kumar, K. (2020). Effect of microwave treatment (low power and varying time) on potato starch: Microstructure, thermo-functional, pasting and rheological properties. *International Journal of Biological Macromolecules*,

155, 27–35.

- Lin, N., Bruzzese, C., & Dufresne, A. (2012). TEMPO-oxidized nanocellulose participating as crosslinking aid for alginate-based sponges. *ACS Applied Materials and Interfaces*, 4(9), 4948–4959.
- Liu, H., Adhikari, R., Guo, Q., & Adhikari, B. (2013). Preparation and characterization of glycerol plasticized (high-amylose) starch-chitosan films. *Journal of Food Engineering*, 116(2), 588–597.
- Luo, Q., Huang, X., Gao, F., Li, D., & Wu, M. (2019). Preparation and characterization of high amylose corn starch-microcrystalline cellulose aerogel with high absorption. *Materials*, 12(9), 1420.
- Luo, Z., He, X., Fu, X., Luo, F., & Gao, Q. (2006). Effect of microwave radiation on the physicochemical properties of normal maize, waxy maize and amylomaize V starches. *Starch/Staerke*, 58(9), 468–474.
- Mehling, T., Smirnova, I., Guenther, U., & Neubert, R. H. H. (2009). Polysaccharide-based aerogels as drug carriers. *Journal of Non-Crystalline Solids*, 355(50–51), 2472–2479.
- Nita, L. E., Ghilan, A., Rusu, A. G., Neamtu, I., & Chiriac, A. P. (2020). New trends in bio-based aerogels. *Pharmaceutics*, 12(5).
- Nordin, N., Othman, S. H., Rashid, S. A., & Basha, R. K. (2020). Effects of glycerol and thymol on physical, mechanical, and thermal properties of corn starch films. *Food Hydrocolloids*, 106, 105884.
- Ollé Resa, C. P., Jagus, R. J., & Gerschenson, L. N. (2014). Effect of natamycin, nisin and glycerol on the physicochemical properties, roughness and hydrophobicity of tapioca starch edible films. *Materials Science and Engineering C*, 40, 281–287.
- Stevenson, D. G., Biswas, A., & Inglett, G. E. (2005). Thermal and pasting properties of microwaved corn starch. *Starch/Staerke*, 57(8), 347–353.
- Takeshita, S., & Yoda, S. (2017). Translucent, hydrophobic, and mechanically tough aerogels constructed from trimethylsilylated chitosan nanofibers. *Nanoscale*, 9(34), 12311–12315.
- Ubeyitogullari, A., Brahma, S., Rose, D. J., & Ciftci, O. N. (2018). In Vitro Digestibility of Nanoporous Wheat Starch Aerogels. *Journal of Agricultural and Food Chemistry*, 66(36),

9490–9497.

- Ubeyitogullari, A., & Ciftci, O. N. (2016). Formation of nanoporous aerogels from wheat starch. *Carbohydrate Polymers*, 147, 125–132.
- Xiao, J., Lv, W., Song, Y., & Zheng, Q. (2018). Graphene/nanofiber aerogels: Performance regulation towards multiple applications in dye adsorption and oil/water separation. *Chemical Engineering Journal*, 338, 202–210.
- Zamora-Sequeira, R., Ardao, I., Starbird, R., & García-González, C. A. (2018). Conductive nanostructured materials based on poly-(3,4-ethylenedioxythiophene) (PEDOT) and starch/ $\kappa$ -carrageenan for biomedical applications. *Carbohydrate Polymers*, 189, 304–312.
- Zheng, Q., Tian, Y., Ye, F., Zhou, Y., & Zhao, G. (2020). Fabrication and application of starch-based aerogel: Technical strategies. *Trends in Food Science & Technology*, 99, 608-620.
- Zhu, F. (2019). Starch based aerogels: Production, properties and applications. *Trends in Food Science & Technology*, 89, 1-10.
- Zhu, J., Hu, J., Jiang, C., Liu, S., & Li, Y. (2019). Ultralight, hydrophobic, monolithic konjac glucomannan-silica composite aerogel with thermal insulation and mechanical properties. *Carbohydrate Polymers*, 207, 246–255.